# The Lateral Diffusion of Selectively Aggregated Peptides in Giant Unilamellar Vesicles

Clarence C. Lee and Nils O. Petersen
Department of Chemistry, The University of Western Ontario, London, Ontario N6A 5B7, Canada

ABSTRACT We have systematically investigated the effect of aggregation of a transmembrane peptide on its diffusion in dimyristoylphosphatidylcholine and in palmitoyloleoylphosphatidylcholine model membranes. The hydrophobic segment of the *b* subunit from *E. coli* $F_1F_0$-ATP synthase was modified with a histidine tag at the carbonyl terminus and was aggregated selectively by using a series of multivalent, dendritic chelating agents with nitrilotriacetic acid functional groups. Peptide complexes ranging from monomers to hexamers were formed and studied in giant unilamellar vesicles. The rate of diffusion for the transmembrane peptide complexes were found to depend on the size of the complex. The results agree with predictions from the free area model for monomers and dimers, and the hydrodynamic continuum model for tetramers, pentamers, and hexamers. Comparisons with diffusion of lipids confirm that the diffusion of a transmembrane peptide is enhanced by coupling of density fluctuations between the two monolayers.

## INTRODUCTION

The lateral diffusion of membrane components within the lipid bilayer is of physiochemical and theoretical interest (Adam and Delbrück, 1968; Clegg and Vaz, 1985), and of biological interest because many biochemical functions may be diffusion controlled (Hackenbrock, 1981; Jans, 1997). For example, the dimerization of tyrosine kinase receptors, such as epidermal growth factor and platelet-derived growth factor, triggers receptor activity and initiates signal transduction. The lateral movement of the receptor proteins to form dimers may be the limiting factor for these cellular processes (Jans, 1997). With more research now focusing on the formation of small lipid domains (Brown and London, 1998a; Rietveld and Simons, 1998; Xu et al., 2001; Yuan et al., 2002) and the association of proteins in small complexes (Brown and London, 1998b; Colledge and Scott, 1999; Simons and Toomre, 2000; Garner et al., 2000; Ikonen, 2001; Pierce, 2002; Zacharias et al., 2002), understanding the lateral diffusion of molecules that form complex structures is of increasing relevance.

Currently, there are two theoretical approaches to explaining the diffusion of amphiphilic molecules in lipid bilayers based on the free area theory (Cohen and Turnbull, 1959; Galla et al., 1979) and the hydrodynamic continuum theory (Saffman and Delbrück, 1975; Hughes et al., 1982; Evans and Sackmann, 1988; Tamm, 1991). Both theoretical and experimental work indicates that the diffusion of molecules in the lipid bilayer should be considered in two regimes (Nir and Stein, 1971). For molecules comparable in size to the solvent molecule, i.e., the phospholipid in the bilayer, the free area theory is the most appropriate model to describe the lateral movement of the diffusant (Derzko and Jacobson, 1980; Vaz et al., 1982b, 1984, 1985a,b; Edidin, 1989). Diffusion of molecules that are large relative to the phospholipid is best explained by the various hydrodynamic continuum models (Chang et al., 1981; Peters and Cherry, 1982; Vaz et al., 1982a, 1984).

Liu and co-workers (Liu et al., 1997) examined the effect of size on the lateral movement of lipid analogs within a monolayer using a series of synthetic macrocyclic polyamide amphiphiles. Their data show that there is a transition between the two theoretical approaches for molecules with a cross-sectional surface area (CSA) of $\sim$1 $nm^2$ at the bilayer surface. In contrast, the size of the molecule within the membrane interior has no effect on the diffusion (Vaz and Hallmann, 1983, Vaz et al., 1985a; Balcom and Petersen, 1993). Thus, from a diffusion perspective, a membrane may be viewed as having three distinct layers: a surface layer on each side being rigid and restricting lipid movement, and a fluid interior layer (Liu et al., 1997). This view is consistent with the gradient in sequential motion from the surface to the interior measured by order parameters or relaxation times in magnetic resonance (Seelig and Seelig, 1974; Petersen and Chan, 1977; Jacobs and Oldfield, 1981; Nagle and Tristram-Nagle, 2000) or fluorescence experiments (Demchenko, 2002). This triple layer model implies that a transmembrane molecule, because it is impeded equally at each surface, should have a diffusion coefficient that is one-half the diffusion rate of a similarly sized molecule that only spans a single leaflet. Using a membrane-spanning phospholipid, Vaz and co-workers (Vaz et al., 1985b) showed that diffusion is faster than expected for a transmembrane, lipid-like molecule. This is attributed to a coupling of density fluctuations between the two lipid monolayers in a membrane. The effect is also predicted to depend on the rigidity of the diffusing molecule (Nadler et al., 1985).

*Submitted July 26, 2002, and accepted for publication September 23, 2002.*

Address reprint requests to Nils O. Petersen, Dept. of Chemistry, The University of Western Ontario, London, ON N6A 5B7, Canada. Tel.: 519-661-3812; Fax: 519-661-3139; E-mail: petersen@uwo.ca.

Clarence C. Lee's present address is Dept. of Chemistry and Biochemistry, University of California, Santa Cruz, CA 95064.



0006-3495/03/03/1756/09 $2.00

In general, the diffusion behavior of lipids, natural proteins, and peptides in a variety of systems are well-understood, but some ambiguities remain. Although there have been studies on the translational diffusion of membrane protein aggregates (Criado et al., 1982; Vaz and Criado, 1985; Kucik et al., 1999), there has been no analogous study involving a single transmembrane peptide. Do peptide dimers move slower relative to the monomer form? Are there differences between receptors with single or multiple transmembrane domains? We therefore reason that a systematic study of aggregate size and its effect on diffusion of a transmembrane peptide would be instructive.

To address this aim, we prepared the short hydrophobic segment of the *b* subunit from *E. coli* $F_1F_0$-ATP synthase with a histidine tag at the carbonyl terminus. The peptide forms an $\alpha$-helical secondary structure with an estimated CSA of 0.5 $nm^2$, established by both computer modeling and heterogeneous Langmuir films. The peptide was also tagged with the fluorescent probe, nitrobenzoxadiazole (NBD), at a lysine residue predicted to be at the membrane surface. Through the histidine tag, we selectively aggregated the peptide with a series of multivalent, dendritic chelating agents containing nitrilotriacetic acid (NTA) groups, to form peptide complexes ranging from monomers to hexamers. The diffusion coefficient for each complex was measured at various temperatures in giant unilamellar vesicles (GUVs) made with either palmitoyloleoylphosphatidylcholine (POPC) or dimyristoylphosphatidylcholine (DMPC).

## MATERIALS AND METHODS

### Materials

The DNA plasmid for the entire *b* subunit and the BL21 C43 *E. coli* strain were obtained from Dr. S. D. Dunn in the Department of Biochemistry at the University of Western Ontario. The plasmid vector, pET 23b, was purchased from Novagen (Darmstadt, Germany). Restriction enzymes, *Nde*I and *Xho*I, were purchased from New England Biolabs (Beverly, MA). All phospholipids were obtained from Avanti Polar Lipids (Alabaster, AL) and were used without further purification. The dendritic chelating agents were prepared by C. Liu (Liu et al., 2002). FLUOREPORTER protein labeling kits for both fluorescein isothiocyanate (FITC) and RHODAMINE RED-X (RRX) were obtained from Molecular Probes (Eugene, OR).

### Peptide preparation

The nucleic acid sequence encoding for the hydrophobic segment of the *b* subunit was isolated and amplified by polymerase chain reaction. The restriction enzymes, *Nde*I and *Xho*I, were used to cut both the appropriate DNA section for the peptide, and the pET 23b plasmid vector. This commercial vector contains the proper genetic coding for the histidine tag. Afterwards, T4 DNA ligase was used to join the two components to form the chimeric vector. The vector was collected and transformed into a mutant strain of *E. coli* BL21, C43 (Miroux and Walker, 1996). The bacteria were grown in 2× YT broth (16 g tryptone, 10 g yeast, and 5 g NaCl in 1 L $H_2O$) with 2 mL of 20 mg/mL ampicillin at 37°C for 12 h. IPTG (isopropyl-1-thio-$\beta$-D-galactopyranoside) was added to the growth to induce the expression of the peptide and the bacteria were cultivated after another 12 h elapsed.

The procedures for the isolation and the purification of the peptide were derived from a method developed by Bligh and Dwyer (1959). The bacteria were homogenized in TE buffer (50 mM Tris, 1 mM EDTA, pH = 8) at a concentration of 10 mL buffer per gram of peptide. The bacteria were ruptured using a French press at 20,000 psi and the resulting solution was centrifuged at 10,000 × g for 20 min. The pellet was resuspended in 1:1 $CHCl_3$/MeOH (chloroform/methanol) solution and centrifuged at 3000 × g for 15 min. The peptide was extracted from the solution using two washings of 1% KCl, with the purified peptide appearing as a white solid at the interface. The solid was collected and was resolubilized in a minimum amount of MeOH. The modified peptide is henceforth referred to as Htm-b.

### Fluorescent derivatization of the peptide

The prescribed procedure from the FLUOREPORTER kits was used to label the peptide with FITC and RRX. The peptide was also labeled with NBD by combining 2 mL of 0.3 mg/mL purified peptide in its original solution with 1 mg of NBD-Cl. Potassium acetate (1 mg) was added to the solution and the reaction was allowed to proceed for eight hours at room temperature. Further purification of the peptide was not pursued because this led to irreversible aggregation of the peptide. The solution was stored at −20°C until the labeled peptide was required. The various derivatized forms of Htm-b are referred to as FITC-b, RRX-b, and NBD-b.

### Langmuir films

Langmuir film experiments were performed on a Kibron $\mu$TROUGH S (Helsinki, Finland). The $\mu$TROUGH S was placed on a Zeiss (Oberkochen, Germany) AXIOVERT microscope with a 32× long distance lens objective for fluorescence microscopy. The AXIOVERT was also equipped with both a FITC filter set ($\lambda_{ex}$ = 450DF55, $\lambda_{em}$ = 535DF55) and a rhodamine filter set ($\lambda_{ex}$ = 560DF40, $\lambda_{em}$ = 600EFLP). Images were collected using an analog Sony (Tokyo, Japan) CCD video camera module with a CMA-02 camera adaptor and digitized into a computer. Dipalmitoylphosphatidylcholine (DPPC), NBD-labeled phosphatidylcholine (NBD-PC), and RRX-b were combined as a 90:1:9 mixture in 3:1 $CHCl_3$/MeOH solution. The solution mixture was added to the corners of the trough, which was filled with doubly distilled and deionized water, until a surface pressure of 0.5 mN/m was attained. Ten minutes of equilibration was provided before compression of the surface film was applied at a rate of 0.5 $Å^2$/chain/min. When a surface pressure of interest was achieved, the compression was stopped and an image of the monolayer was recorded.

### Preparation of peptide aggregates

The methodology for the aggregation of histidine-tagged peptides was developed by Liu et al. (2002). Stock solutions of each chelating agent were prepared in millimolar concentrations using doubly distilled and deionized water. The three largest chelating agents required heating for several minutes to dissolve. Stock solutions at 1 mM of either $NiCl_2$ or $NiSO_4$ were used as the source for divalent cations. To coordinate the $Ni^{2+}$ with the various chelators, the stock $Ni^{2+}$ solutions and each chelating agent were mixed in appropriate ratios and allowed to equilibrate for one hour. The resulting aggregation agent solutions of micromolar concentrations were stored at 4°C.

The aggregation agents were used as the limiting reagent in mixtures with NBD-b in its $CHCl_3$/MeOH solution to form each complex. The ratios of NBD-b to aggregation agent necessary for successful formation of the specific aggregates were determined in solution with a histidine-tagged hydrophilic protein, thioredoxin (Liu et al., 2002). The resulting mixtures of NBD-b and aggregation agent, at a final volume of 2 mL, were allowed to sit overnight at 4°C before use.

### Vesicle preparation

GUVs of DMPC and the peptide aggregates were prepared at 35°C by the electroformation method (Angelova and Dimitrov, 1986; Dimitrov and

Angelova, 1987; Angelova et al., 1992; Bagatolli and Gratton, 1999) using a homebuilt device (Vanstone, London, ON, Canada). The device consists of two parallel platinum wires (1-mm diameter) held horizontally within a brass ring. Vacuum grease was used to seal an 18-mm diameter glass cover slip at the bottom of the ring to form the chamber floor. The brass ring was used to control the temperature of the chamber through a Cambion Bipolar temperature controller (Cambion Division of Midland Ross, Brampton, ON, Canada).

The solutions used to form the GUVs consist of 0.3 mg/mL phospholipid with either 0.5 mol% NBD labeled phosphatidylethanolamine (NBD-PE) or 0.5 mol% NBD-b in 3:1 $CHCl_3$/MeOH. The latter peptide concentration for the mixture was also used for the formation of GUVs with peptide clusters. Using the prescribed electroformation method resulted in vesicles with a mean diameter of 30 $\mu$m.

## Diffusion measurements

Diffusion measurements of NBD-b and the peptide aggregates were performed by fluorescence photobleaching recovery (FPR). The system used for this work is a homebuilt system that has been described previously (Petersen et al, 1986; Liu et al., 1997). With a 40× water immersion lens, a laser beam radius of 0.92 $\mu$m was measured in the focal plane by using the gold edge method in conjunction with a homebuilt microscope stage subassembly (McConnaughey, St. Louis, MO). Vesicles with a minimum diameter of 20 $\mu$m were selected for the diffusion measurements. Once a suitable GUV was found, it was aligned along the optical axis and the laser beam was focused on the surface of the vesicle. The FPR measurements and the fitting of the data were performed as reported previously (Edidin et al., 1976; Axelrod et al., 1976; Axelrod, 1985; Petersen et al, 1986).

## RESULTS

The DNA encoding for Htm-b was shown to be correct by DNA sequencing. Purified Htm-b was characterized by mass spectroscopy, gel electrophoresis, and amino acid analysis (Alberta Peptide Institute, University of Alberta, Canada). The amino acid sequence for the modified peptide is shown below.

MNL**NATILGQAIAFVLFVLFCM**KYLEHHHHHH

The sequence corresponding to the hydrophobic segment of the *b* subunit is underlined. Residues 4-22 (boldface type) are believed to span the hydrophobic portion of the lipid bilayer (Dmitriev et al., 1999). Circular dichroism confirmed that, like the native species, our modified peptide adopts an $\alpha$-helical conformation. The shape of the Htm-b molecule was modeled using HYPERCHEM 6.03 (Hypercube, Gainsville, FL), with the results shown in Fig. 1. From the computer model, it is apparent that Htm-b has a CSA that varies along the length of the molecule and the molecule is not cylindrical. The approximate surface area is estimated as 0.55 $nm^2$, assuming a rotationally averaged cylindrical shape. An experimental, indirect estimate of the CSA for Htm-b was obtained by studying the mixing of phospholipid (DPPC) and fluorescently labeled Htm-b in monolayer systems as a function of pressure. Fluorescent images of a monolayer containing DPPC, RRX-b, and NBD-PC are shown in Fig. 2. In Fig. 2 *A*, the fluorescent emission from RRX-b shows that at low pressures, the peptide resides in the

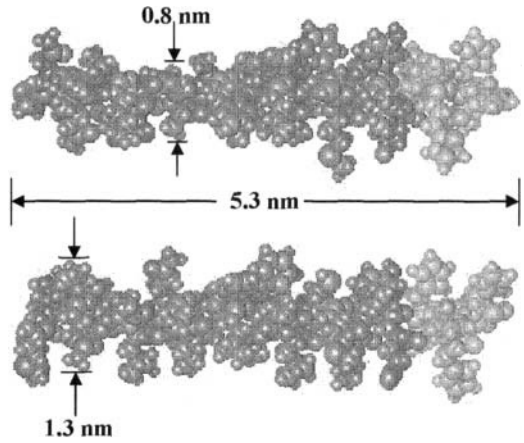


FIGURE 1 Computer model of Htm-b at two different rotations. The images show Htm-b with the histidine amino acids at the carbonyl terminus (*light gray*). The simulations show that the length of the peptide is 5.3 nm. The variability of the peptide diameter along the hydrophobic segment of the *b* subunit is evident. The average cross-sectional area in the hydrophobic region is estimated at 0.5 $nm^2$.

continuous, liquid expanded (LE) region of the DPPC monolayer. The dark circular regions correspond to liquid condensed (LC) DPPC domains, which exclude the dye labeled peptide and the dye labeled lipid, NBD-PC (Hollars and Dunn, 1998). As surface pressure increases from 5 mN/m to 30 mN/m, the fluorescence in the LC domains increases relative to the fluorescence in the LE region, indicating an increased relative partition of the peptide into the LC domains (Fig. 2, *B–E*). At 30 mN/m, the pressure estimated for biological membranes (Nagle, 1976; Liu et al., 1997; Feng, 1999; Yuan et al., 2002), the partitioning of the peptide between the two regions is nearly equal because the domains are no longer distinguishable. Note that the corresponding NBD-PC emission image (Fig. 2 *F*) shows that the LC domains still exclude the NBD-PC at this pressure and that their number, size, and shape are consistent with previous work. (Peters and Beck, 1983; McConnell et al., 1984; Hollars and Dunn, 1998).

The data in Fig. 2 show that the peptide partitions well into the LC domains of the monolayer at 30 mN/m. The phospholipids in these domains are tightly packed in a near solid lattice structure. To partition well into the LC phase without disrupting the lattice, the peptide must have a CSA similar to the host lipid. The surface area of DPPC in its liquid condensed state is ~0.5 $nm^2$ at 30 mN/m (Vaz et al., 1985a; Nagle and Tristram-Nagle, 2000). Thus, we conclude that the peptide has an effective cross-sectional surface area of 0.5 $nm^2$. This value agrees with the molecular modeling and will therefore be used in the rest of the discussions.

The incorporation of derivatized Htm-b into GUVs of DMPC and POPC was visualized using confocal microscopy. An example of NBD-b incorporation into a POPC GUV is shown in Fig. 3. The fluorescence is clearly confined to the membrane, which, by all accounts, is a single bilayer

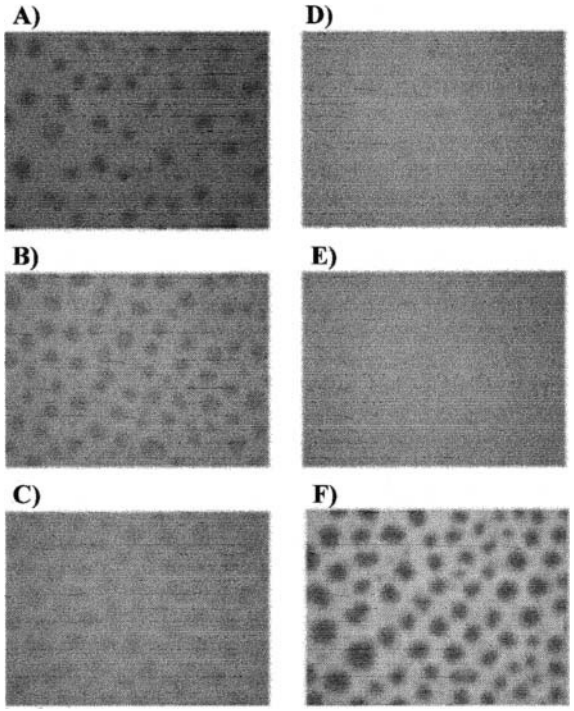


FIGURE 2 Images of a mixed monolayer system containing 90:1:9 DPPC/RRX-b/NBD-PC measured through a rhodamine filter set (*A–E*) and FITC filter set (*F*) at various surface pressures. Each image is 481 $\mu$m $\times$ 642 $\mu$m. Images of the Langmuir film were recorded through the rhodamine filter set at 10 mN/m (*A*); 15 mN/m (*B*); 20 mN/m (*C*); 25 mN/m (*D*); and 30 mN/m (*E*). As surface pressure increases, the contrast between the brighter LE region and the darker lipid LC domains is reduced. Examination of the same film using the FITC filter set at 30 mN/m (*F*) reveals the continued presence of LC domains, suggesting that the contrast reduction seen from images *A–E* arises because RRX-b is able to partition into the liquid condensed regions at higher pressures.

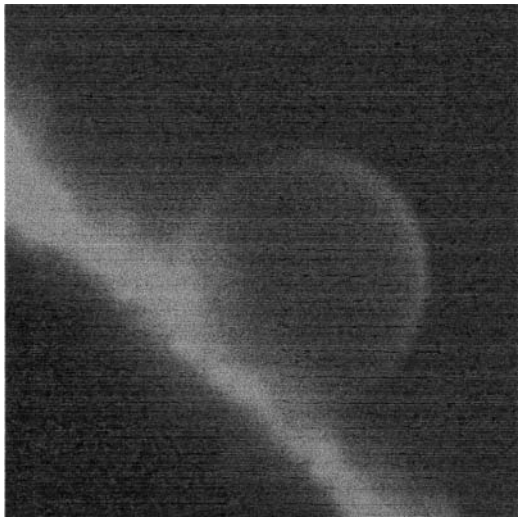

FIGURE 3 Confocal image showing the incorporation of a derivatized peptide, RRX-b, into POPC GUVs at 20°C. The GUVs were created using the electroformation method. After formation, the vesicles remain attached to the platinum wire, which is located at the bottom left corner of the image. The image size is 69 $\mu$m $\times$ 69 $\mu$m and the large GUV in the center is ~40 $\mu$m in diameter.

(Méléard et al., 1997). The incorporation was confirmed qualitatively by observing fluorescence resonance energy transfer between derivatized phospholipid and labeled peptide at high concentration (data not shown). At Htm-b concentration levels used for the photobleaching measurements, no energy transfer was detected between donor (FITC) and acceptor (RRX) labeled Htm-b when they were mixed in the vesicles. This implies that the peptide does not self-associate at low concentration and thus, only the monomeric species were incorporated in the lipid bilayers under normal conditions.

The methodology used to control peptide aggregation is based on the principles of metal affinity chromatography (Porath et al., 1975). Liu et al. synthesized a series of multivalent chelating agents composed of macrocyclic amide rings with dendritic arms (Liu et al., 2002). As seen in Fig. 4, each dendritic arm terminates with an NTA functional group. The NTA group can coordinate with divalent cations, such as $Ni^{2+}$, and occupy four of the six coordination sites on the cation. In turn, two imidazole groups in the histidine tag of the peptide can bind to the two remaining sites. The resulting peptide-Ni-NTA complex is very stable and is, in effect, quantitative and stoichiometric. The size of the macrocyclic ring determines the number of NTA groups and hence the number of peptides bound into a single complex. The multivalent, dendritic chelators shown in Fig. 4 can selectively produce dimers, trimers, tetramers, pentamers, or hexamers of any histidine-tagged protein or peptide. The complex can be dissociated by adding excess amounts of a competing agent, such as EDTA, or free imidazole. This reversibility to monomers, in principle, allows comparative studies between aggregate and monomer in the same system.

NBD-b was studied using FPR, with the diffusion coefficients for the monomeric species and the specific peptide clusters determined in DMPC GUVs at 35°C. The lateral diffusion of NBD-PE was measured for comparison. The diffusion coefficients for the complexes relative to NBD-PE are shown in Fig. 5 as a function of the estimated CSA for each species. There is a clear dependence of the diffusion rate on the cross-sectional surface area. The mobile fraction, $X_m$, was close to unity in all cases, which allowed for multiple measurements on the same vesicle. On average, ten measurements were performed on each GUV. The mean $\pm$ SE at 99% confidence level is shown for each of the mean diffusion values.

Fig. 5 shows that the diffusion coefficient of the peptide and the specific aggregates varies with the molecular size. The diffusion rate for monomeric NBD-b and the dimeric species are comparable. The trimer moves more slowly, whereas the tetramer, pentamer, and hexamer move the slowest. The three largest aggregates all move at 40% of the

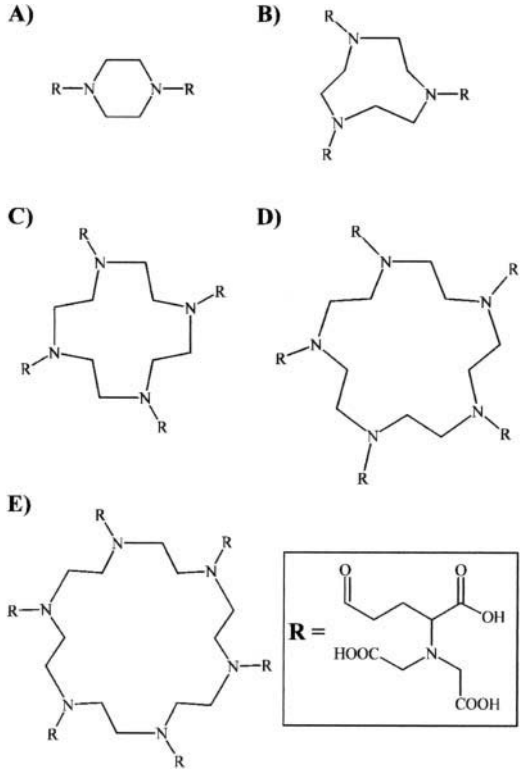


FIGURE 4 Molecular structures of the dendritic chelating agents (Liu et al., 2002): dimer agent (*A*); trimer agent (*B*); tetramer agent (*C*); pentamer agent (*D*); and hexamer agent (*E*). Note that each branch originates at a nitrogen in the ring and terminates with a nitrilotriacetic acid group used to complex with nickel to the histidine tag. The valency of the complexing agent therefore is governed by the number of nitrogens in the ring.

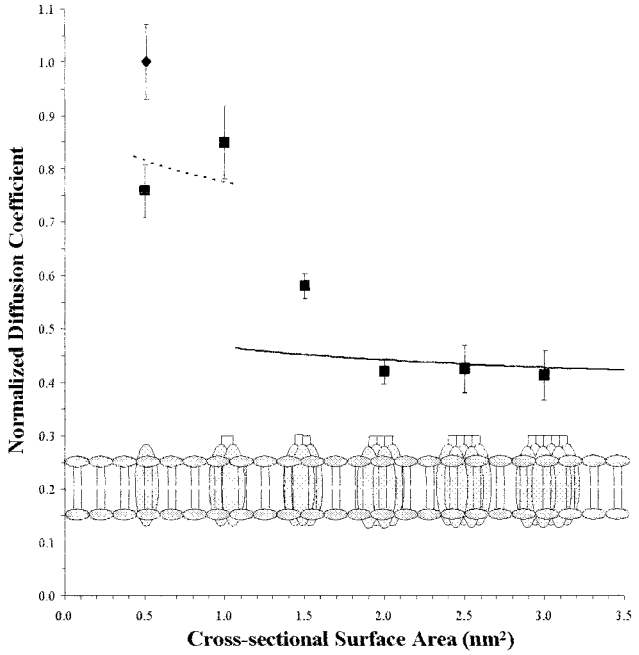


FIGURE 5 Normalized diffusion coefficient plotted as a function of the cross-sectional surface area for Htm-b and the peptide aggregates in DMPC bilayers at 35°C. Diffusion coefficients for the transmembrane diffusants (■) are normalized with the diffusion coefficient for NBD-PE (♦). The schematic representation of the state of aggregation of the transmembrane diffusants in the lipid bilayer is shown for each data point at the bottom of the graph. The error bars represent the mean ± SE at 99% confidence level. Theoretical calculations are shown for the free area theory (*solid line*) and the Saffman-Delbrück hydrodynamic model (*dashed line*). The calculations were performed with the following fixed parameters: $\gamma a^*/a_0 = 0.4$, $\beta = 0.148$, $\alpha_a = 2.3 \times 10^{-3}\ K^{-1}$, $T_m = 23.9°C$, $h = 3.0$ nm, $\mu_w = 0.00728$ Poise, $\mu_m = 1.75$ Poise.

diffusion rate for the phospholipid. The grouping of the diffusion rates is similar to that observed for the lipid analogs of comparable sizes (Liu et al., 1997). This suggests that the diffusion of NBD-PE, NBD-b monomer, and the dimer should be interpreted by the free area theory, whereas the movement of the three largest oligomers should be represented by the hydrodynamic, or continuum theory. The calculations based on these diffusion theories using reasonable adjustable parameters (see below) are also shown in Fig. 5.

A diffusion coefficient interpreted by the interfacial viscosity limited free area theory may be calculated using Eq. 1 (Vaz et al., 1985a,b),

$$D = (kT/f)\exp[(-\gamma a^*)/(a_o[\beta + \alpha_a(T - T_m)])], \quad (1)$$

where $k$ is Boltzmann's constant, $T$ is temperature, $f$ is a translational friction coefficient representing the interactions at the membrane-water interface and within the interior of the bilayer, $\gamma$ is a numerical factor that accounts for free area overlap ($\gamma$ has values between 0.5 and 1.0), $a^*$ is the critical free area, $a_0$ is the van der Waals area per lipid molecule, $\alpha_a$ is the lateral thermal expansion coefficient in the liquid-crystalline phase, $T_m$ is the main phase transition temperature for the lipid bilayer, and $a_0\beta$ is the free area at the $T_m$ (Vaz et al., 1985a).

In Fig. 5, the calculations assume that $\gamma a^*/a_0 = 0.4$, $\beta = 0.148$, $\alpha_a = 2.3 \times 10^{-3}\ K^{-1}$ and $T_m = 23.9°C$ for DMPC bilayers (Galla et al., 1979; Vaz et al., 1985a, 1985b). The friction coefficient was considered to contain two terms, $f = 2f_1 + f_2$, with $f_1$ due to the interaction at the lipid-water interface, and $f_2$ due to the lipid tails within the interior of the membrane. A factor of two is used to account for the peptide being in contact with the aqueous phase on both sides of the bilayer. The friction coefficient at the bilayer-water interface has the form $f_1 = 4\pi\mu_w R$, where $R$ is the radius of the diffusing particle and $\mu_w$ is the viscosity of water at 35°C. In contrast, $f_2$ is difficult to estimate because it is dependent on both the viscosity within the membrane and the effective size of the phospholipid acyl chains. Thus, $f_2$ was used in our calculation as an adjustable parameter. A value of $5 \times 10^{-11}$ Ns/m was needed to match the calculations with the experimental diffusion rate. For comparison, $f_2 = \sim 4 \times 10^{-11}$ Ns/m for NBD-PE (Vaz et al., 1985a) and for small lipid analogs (Liu et al., 1997). Also, $f_2$ for a transmembrane lipid was found to be 15% greater than the value determined

for NBD-PE (Vaz et al., 1985b), which compares favorably with the coefficient determined for our peptide monomers and dimers. Interestingly, the parameters used to describe NBD-PE diffusion could be applied equally for both NBD-b monomers and dimers. Although the interfacial viscosity limited free area theory was designed to describe the diffusion for lipid-like molecules in one leaflet of the bilayer, it appears to describe the diffusion of a transmembrane molecule equally well.

The hydrodynamic model, proposed by Saffman and Delbrück (1975), describes the lateral diffusion of a cylinder in a thin viscous sheet, such as a membrane-spanning protein in a lipid bilayer, using Eq. 2.

$$D = (kT/4\pi\mu_m h)[\ln(\mu_m h/\mu_w R) - \gamma] \quad (2)$$

The parameters, $\mu_w$ and $\mu_m$, are the viscosities of the surrounding media and the membrane respectively, $h$ is the thickness of the viscous sheet, $R$ is the radius of the diffusant, and $\gamma$ is Euler's constant. The approach proposed by Evans and Sackmann (1988) for asymmetric membrane environments yield comparable results in this and other systems (Liu et al., 1997).

The membrane viscosity used for the theoretical calculation is estimated at 1.75 Poise, based on the viscosity of DMPC determined at 32°C (Peters and Cherry, 1982). As seen in Fig. 5, the results from the Saffman and Delbrück model compares favorably with the experimental data provided a membrane thickness of 3.0 nm is used rather than the 5 nm typically assumed for this calculation (Clegg and Vaz, 1985; Saxton, 1999). This suggests that the region(s) of the bilayer that resists movement is thinner than the entire membrane.

The lateral diffusion coefficients of NBD-PE, NBD-b, and the tetramer aggregate were also studied in POPC GUVs at temperatures between 9°C and 35°C. The apparent activation energy for each of the complexes were determined from the resulting linear Arrhenius plots and are listed in Table 1.

The activation energy for the monomeric species is comparable to the lipid probe and is similar to previous measurements for lipids and small lipids analogs (Vaz et al., 1982a; Liu et al., 1997). The activation energy for the tetramer species is significantly lower and compares very well with the values obtained for lipid analogs of similar cross-sectional surface areas (Liu et al., 1997). The data confirm that the activation energy of small molecules is larger than that of large molecules. This presumably reflects the different physical processes that control the diffusion in each size regime; density fluctuations for the small molecules and viscous drag for the larger molecules.

**TABLE 1 Apparent activation energies for peptide complexes in POPC**

| Complex | $E_a$ (kJ/mol) |
|---|---|
| NBD-PE | 39.6 ± 4.1 |
| NBD-b | 39.5 ± 3.8 |
| Tetramer | 24.9 ± 3.8 |

Errors represent the mean ± SE at the 99% confidence level.

## DISCUSSIONS

The experiments in this manuscript demonstrate that a modified hydrophobic peptide can be selectively aggregated and the lateral diffusion of the resulting species can be studied in GUVs using photobleaching methods. The lateral diffusion depends on the size and shape of the molecules because it depends on the degree of peptide clustering. The diffusion of the monomer and dimer species can be described by the free area theory, whereas the tetramer, pentamer, and hexamer diffusion coefficients are compatible with the Saffman-Delbrück hydrodynamic continuum model.

The general trend in diffusive behavior observed here for a transmembrane peptide and its selectively aggregated complexes parallels that observed by Liu et al. (1997) with macrocyclic polyamide amphiphiles in monolayers. A discontinuity is observed in both experimental data sets, suggesting that the transition between the two diffusion regimes occurs for molecules with cross-sectional surface areas from 0.8 $nm^2$ to 1 $nm^2$. Interestingly, the results for the trimeric complex appear to be in the transition region, suggesting that both solvent density fluctuations and viscous drag affect the diffusion rate.

Correspondingly, lipid analogs with a 1-$nm^2$ CSA also exhibit intermediate behavior and may therefore also be in the middle of the transition region (Liu et al., 1997). The difference in activation energy between small and large molecular systems supports the idea that the diffusion is controlled by a different physical process in each of the two size regimes. It is particularly reassuring that corresponding differences are seen with both the monolayer (Liu et al., 1997) and the transmembrane probes (Vaz et al., 1985b).

To compare the diffusion of a molecule in a monolayer with one in a bilayer, we examine the ratio of their diffusion coefficients with the predicted ratio, assuming that a simple additive effect predicted by the triple layer model is applicable. Fig. 6 *A* shows the average diffusion coefficients for small lipid analogs (Liu et al., 1997) and for peptide monomers and dimers relative to NBD-PE. The lipid analogs diffuse as fast as the lipid, but the transmembrane peptides move at 80% of this rate, rather than at 50% as predicted if the two bilayer leaflets acted independently. Similarly, a higher than expected diffusion coefficient has been observed for a transmembrane lipid probe, which was reported to move at ~65% of the lipid rate (Vaz et al., 1985b).

The phenomenon has been rationalized by Nadler et al. (1985), who suggested that the transmembrane molecule couples density fluctuations in one monolayer to the other within a membrane. This coupling is a result of the transmembrane molecule strongly preferring its long axis

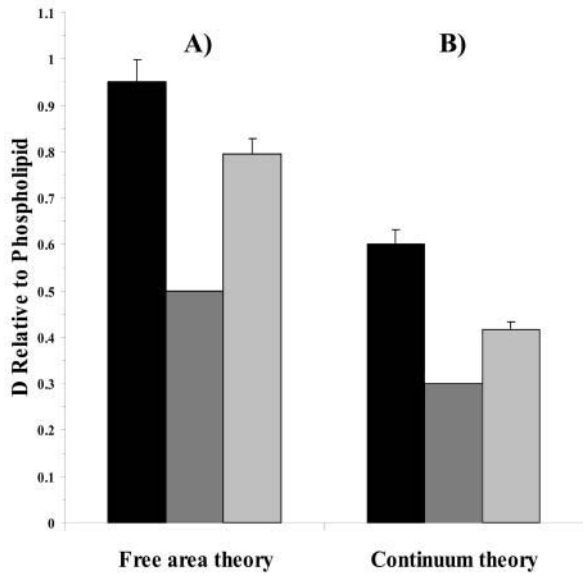


FIGURE 6 Comparison of mean diffusion coefficients for monolayer diffusants (polyamide amphiphiles) (*black bar*) and bilayer-spanning diffusants (peptide aggregates) (*light gray bar*) in DMPC at 35°C, with the corresponding values predicted by the triple layer model (*cross-hatched bar*). The data are averages normalized to the diffusion rate for NBD-PE under the same conditions. (*A*) corresponds to monomers and dimers reflecting the free area theory and (*B*) corresponds to the larger molecules or complexes reflecting the continuum theory. In both cases, the predicted diffusion is slower than the observed diffusion, suggesting some interaction between the two monolayers.

to stay perpendicular to the plane of the lipid bilayer. The prediction is that the coupling effect is greater when the transmembrane molecule is more rigid, which would explain why the peptide monomers and dimers have a faster diffusion rate compared to the transmembrane lipid probe.

Fig. 6 *B* shows the average diffusion coefficients of large lipid analogs (Liu et al., 1997) and for the peptide tetramers, pentamers, and hexamers relative to the NBD-PE diffusion rate. The data emphasize that the larger molecules move more slowly, but once again, the transmembrane clusters diffuse more rapidly than predicted if viscosity effects within the membrane were simply additive. This effect, which is less pronounced for these complexes than for the monomers or the dimers, has not been observed before. There are two possible rationales. First, it is possible that the large lipid analogs are moving relatively slower because of interactions between the two monolayers, leading to the lower predicted value for the transmembrane unit. Second, the transmembrane peptide complexes may be sufficiently flexible and porous to allow lipids to diffuse in and out of their molecular structures.

In summary, the diffusion of a molecule with CSA comparable to the lipid solvent is governed by density fluctuations, whether it resides in a single monolayer only or traverses the entire bilayer. The activation energies are comparable, suggesting that the same fundamental physical forces control the diffusion. The relatively fast diffusion of the transmembrane peptide monomer and dimer suggests that the density fluctuations in one monolayer induce fluctuations in the other, enhancing the probability for a diffusive hop. Correspondingly, a molecule with CSA above $\sim$1 nm$^2$ moves more slowly than the lipid, whether they reside in a monolayer only or span the bilayer. The activation energies are smaller for these molecules, confirming that different physical forces regulate their diffusion rates.

This work raises several biologically relevant issues. Membrane proteins often have either one transmembrane domain, as in tyrosine kinase receptors, or seven transmembrane domains, as in G-protein coupled receptors. Our data suggest that this difference in tertiary structure alone will segregate these membrane proteins into two different diffusion classes as well. The importance of having a single transmembrane domain versus seven transmembrane domains could therefore relate to the speed with which proteins can interact and initiate a signal transduction event. The diffusion rates for monomers and dimers of single transmembrane proteins are the same. Correspondingly, the diffusion rates for monomers and dimers of the larger multiple transmembrane proteins would be the same. This implies that simple dimerization of receptors of either type during signal transduction would not alter their diffusion rate and hence, should not be a rate limiting factor for subsequent diffusion dependent processes.

Although the relation between degree of aggregation and diffusion rate is clear in these model membranes, it remains true that cell membranes are structurally heterogeneous. Protein-protein (Duband et al., 1988; Jans, 1997; Colledge and Scott, 1999; Garner et al., 2000) and protein-lipid interactions (Pierce, 2002; Zacharias et al., 2002), confinement due to the cytoskeleton (Tsuji and Ohnishi, 1986; Tsuji et al., 1988; Kusumi et al., 1993; Kusumi and Sako, 1996; Sako and Kusumi, 1994, 1995), and lipid rafts (Glaser, 1993; Brown and London, 1998a,b; Ikonen, 2001) are all examples of membrane heterogeneity which may affect the long distance diffusion dynamics within the lipid bilayer. Nevertheless, it is possible that the dynamics of protein-protein interactions over short distances within domains is controlled by the diffusion processes described in this work.

We are grateful to Dr. Matt Revington for assistance with preparation of the Htm-b peptide and to Dr. Matt Revington and Dr. Stan Dunn for stimulating discussions about the project.

The work was supported by an operating grant from the Natural Sciences and Engineering Research Council, Canada (NOP).

## REFERENCES

Adam, G., and M. Delbrück. 1968. Reduction of dimensionality in biological diffusion processes. *In* Structural Chemistry and Molecular Biology. A. Rich and N. Davidson, editors. W. H. Freeman and Company, San Francisco. 198–215.

Angelova, M. I., and D. S. Dimitrov. 1986. Liposome electroformation. *Faraday Discuss. Chem. Soc.* 81:303–311.

Angelova, M. I., S. Soléau, Ph. Meléard, J. F. Faucon, and P. Bothorel. 1992. Preparation of giant vesicles by external AC fields: kinetics and application. *Prog. Colloid Polym. Sci.* 89:127–131.

Axelrod, D. 1985. Fluorescence photobleaching techniques and lateral diffusion. *In* Spectroscopy and the Dynamics of Molecular Biological Systems. P. Bayley and R. Dale, editors. Academic Press, London. 163–176.

Axelrod, D., D. E. Koppel, J. Schlessinger, E. Elson, and W. W. Webb. 1976. Mobility measurement by analysis of fluorescence photobleaching recovery kinetics. *Biophys. J.* 16:1055–1069.

Bagatolli, L. A., and E. Gratton. 1999. Two-photon fluorescence microscopy observation of shape changes at the phase transition in phospholipid giant unilamellar vesicles. *Biophys. J.* 77:2090–2101.

Balcom, B. J., and N. O. Petersen. 1993. Lateral diffusion in model membranes is independent of the size of the hydrophobic region of molecules. *Biophys. J.* 65:630–637.

Bligh, E. G., and W. J. Dwyer. 1959. A modified method of total lipid extraction and purification. *Can. J. Biochem. Physiol.* 37:911–916.

Brown, D. A., and E. London. 1998a. Structure and origin of ordered lipid domains in biological membranes. *J. Membr. Biol.* 164:103–114.

Brown, D. A., and E. London. 1998b. Functions of lipid rafts in biological membranes. *Annu. Rev. Cell Dev. Biol.* 14:111–136.

Chang, C. H., H. Takeuchi, T. Ito, K. Machida, and S. Ohnishi. 1981. Lateral mobility of erythrocyte membrane proteins studied by the fluorescence photobleaching recovery technique. *J. Biochem.* 90: 997–1004.

Clegg, R. M., and W. L. C. Vaz. 1985. Translational diffusion of proteins and lipids in artificial lipid bilayer membranes. A comparison of experiment with theory. *In* Progress in Protein-Lipid Interactions. A. Watts and J. J. H. M. Dupont, editors. Elsevier Science Publishing, Amsterdam. 173–229.

Cohen, M. H., and D. Turnbull. 1959. Molecular transports in liquids and gases. *J. Chem. Phys.* 31:1164–1169.

Colledge, M., and J. D. Scott. 1999. AKAPs: from structure to function. *Trends Cell Biol.* 9:216–221.

Criado, M., W. L. C. Vaz, F. J. Barrantes, and T. M. Jovin. 1982. Translational diffusion of acetylcholine receptor (monomeric and dimeric forms) of *Torpedo marmorata* reconstituted into phospholipid bilayers studied by fluorescence recovery after photobleaching. *Biochemistry.* 21:5750–5755.

Demchenko, A. P. 2002. The red-edge effects: 30 years of exploration. *Luminescence.* 17:19–42.

Derzko, Z., and K. Jacobson. 1980. Comparative lateral diffusion of fluorescent lipid analogues in phospholipid multibilayers. *Biochemistry.* 19:6050–6057.

Dmitriev, O., P. C. Jones, W. P. Jiang, and R. H. Fillingame. 1999. Structure of the membrane domain of subunit *b* of the *Escherichia coli* $F_0F_1$ ATP synthase. *J. Biol. Chem.* 274:15598–15604.

Dimitrov, D. S., and M. J. Angelova. 1987. Lipid swelling and liposome formation on solid surfaces in external electric fields. *Prog. Colloid Polym. Sci.* 73:48–56.

Duband, J.-L., G. H. Nuckolls, A. Ishihara, T. Hasegawa, K. M. Yamada, J. P. Thiery, and K. Jacobson. 1988. Fibronectin receptor exhibits high lateral mobility in embryonic locomoting cells but is immobile in focal contacts and fibrillar streaks in stationary cells. *J. Cell Biol.* 107: 1385–1396.

Edidin, M., Y. Zagyansky, and T. J. Lardner. 1976. Measurement of membrane protein lateral diffusion in single cells. *Science.* 191:466–468.

Edidin, M. 1989. Rotational and lateral diffusion of membrane proteins and lipids: phenomena and function. *Curr. Top. Membr. Transp.* 29:91–127.

Evans, E., and E. Sackmann. 1988. Translational and rotational drag coefficients of a disk moving in a liquid membrane associated with a rigid substrate. *J. Fluid Mech.* 194:553–561.

Feng, S.-S. 1999. Interpretation of mechanochemical properties of lipid bilayer vesicles from the equation of state or pressure-area measurements of the monolayer at the air-water or oil-water interface. *Langmuir.* 15:998–1010.

Galla, H. J., W. Hartmann, U. Theilen, and E. Sackmann. 1979. On two-dimensional passive random walk in lipid bilayers and fluid pathways in biomembranes. *J. Membr. Biol.* 48:215–236.

Garner, C. C., J. Nash, and R. L. Huganir. 2000. PDZ domains in synapse assembly and signalling. *Trends Cell Biol.* 10:274–280.

Glaser, M. 1993. Lipid domains in biological membranes. *Curr. Opin. Struct. Biol.* 3:475–481.

Hackenbrock, C. R. 1981. Lateral diffusion and electron transfer in the mitochondrial inner membrane. *Trends Biochem. Sci.* 6:151–154.

Hollars, C. W., and R. C. Dunn. 1998. Submicron structure in L-$\alpha$-dipalmitoylphosphatidylcholine monolayers and bilayers probed with confocal, atomic force, and near-field microscopy. *Biophys. J.* 75: 342–353.

Hughes, B. D., B. A. Pailthorpe, L. R. White, and W. H. Sawyer. 1982. Extraction of membrane microviscosity from translational and rotational diffusion coefficients. *Biophys. J.* 37:673–676.

Ikonen, E. 2001. Roles of lipid rafts in membrane transport. *Curr. Opin. Cell Biol.* 13:470–477.

Jacobs, R. E., and E. Oldfield. 1981. NMR of membranes. *Progress in Nuclear Magnetic Resonance Spectroscopy.* 14:113–136.

Jans, D. A. 1997. The Mobile Receptor Hypothesis: The Role of Membrane Receptor Lateral Movement in Signal Transduction. Chapman & Hall, Austin.

Kucik, D. F., E. L. Elson, and M. P. Sheetz. 1999. Weak dependence of mobility of membrane protein aggregates on aggregate size supports a viscous model of retardation of diffusion. *Biophys. J.* 76:314–322.

Kusumi, A., Y. Sako, and M. Yamamoto. 1993. Confined lateral diffusion of membrane receptors as studied by single particle tracking (nanovid microscopy). Effects of calcium-induced differentiation in cultured epithelial cells. *Biophys. J.* 65:2021–2040.

Kusumi, A., and Y. Sako. 1996. Cell surface organization by the membrane skeleton. *Curr. Opin. Cell Biol.* 8:566–574.

Liu, C., A. Paprica, and N. O. Petersen. 1997. Effects of size of macrocyclic polyamides on their rate of diffusion in model membranes. *Biophys. J.* 73:2580–2587.

Liu, C., R. H. E. Hudson, and N. O. Petersen. 2002. Convergent and sequential synthesis of dendritic, multivalent complexing agents. *Synthesis.* 10:1398–1406.

McConnell, H. M., L. K. Tamm, and R. M. Weiss. 1984. Periodic structures in lipid monolayer phase transitions. *Proc. Natl. Acad. Sci. USA.* 81:3249–3253.

Méléard, P., G. Grebeaud, T. Pott, L. Fernandez-Puente, I. Bivas, M. D. Mitov, J. Dufourcq, and P. Bothorel. 1997. Bending elasticities of model membranes: influences of temperature and sterol content. *Biophys. J.* 72:2616–2629.

Miroux, B., and J. E. Walker. 1996. Over-production of proteins in *Escherichia* coli: mutant hosts that allow synthesis of some membrane proteins and globular proteins at high levels. *J. Mol. Biol.* 260:289–298.

Nadler, W., P. Tavan, and K. Schulten. 1985. A model for the lateral diffusion of stiff chains in a lipid bilayer. *Eur. Biophys. J.* 12:25–31.

Nagle, J. F. 1976. Theory of monolayer and bilayer phase transition: effect of headgroup interactions. *J. Membr. Biol.* 27:233–250.

Nagle, J. F., and S. Tristram-Nagle. 2000. Structure of lipid bilayers. *Biochim. Biophys. Acta.* 1469:159–195.

Nir, S., and W. D. Stein. 1971. Two modes of diffusion in liquids. *J. Chem. Phys.* 55:1598–1603.

Peters, R., and K. Beck. 1983. Translational diffusion in phospholipid monolayers measured by fluorescence microphotolysis. *Proc. Natl. Acad. Sci. USA.* 80:7183–7187.

Peters, R., and R. J. Cherry. 1982. Lateral and rotational diffusion of Bacteriorhodopsin in lipid bilayers: experimental test of the Saffman-Delbrück equations. *Proc. Natl. Acad. Sci. USA*. 79:4317–4321.

Petersen, N. O., and S. I. Chan. 1977. More on the motional state of lipid bilayer membranes: interpretation of order parameters obtained from nuclear magnetic resonance experiments. *Biochemistry*. 16:2657–2667.

Petersen, N. O., S. Felder, and E. L. Elson. 1986. Measurement of lateral diffusion by fluorescence photobleaching recovery. *In* Handbook of Experimental Immunology. D. M. Weir, editor. Blackwell, Edinburgh. 24.1–24.3.

Pierce, S. K. 2002. Lipid rafts and B-cell activation. *Nat. Rev. Immunol.* 2:96–105.

Porath, J., J. Carlsson, I. Olsson, and G. Belfrage. 1975. Metal chelate affinity chromatography, a new approach to protein fractionation. *Nature*. 258:598–599.

Rietveld, A., and K. Simons. 1998. The differential miscibility of lipids as the basis for the formation of functional membrane rafts. *Biochim. Biophys. Acta*. 1376:467–479.

Saffman, P. G., and M. Delbrück. 1975. Brownian motion in biological membranes. *Proc. Natl. Acad. Sci. USA*. 72:3111–3113.

Sako, Y., and A. Kusumi. 1994. Compartmentalized structure of the plasma membrane for receptor movements as revealed by a nanometer-level motion analysis. *J. Cell Biol.* 125:1251–1264.

Sako, Y., and A. Kusumi. 1995. Barriers for lateral diffusion of transferrin receptor in the plasma membrane as characterized by receptor dragging by laser tweezers: fence versus tether. *J. Cell Biol.* 129:1559–1574.

Saxton, M. J. 1999. Lateral diffusion of lipids and proteins. *Curr. Topics Membr.* 48:229–282.

Seelig, A., and J. Seelig. 1974. The dynamic structure of fatty acyl chains in a phospholipid bilayer measured by deuterium magnetic resonance. *Biochemistry*. 13:4839–4845.

Simons, K., and D. Toomre. 2000. Lipid rafts and signal transduction. *Nat. Rev. Mol. Cell Biol.* 1:31–39.

Tamm, L. K. 1991. Membrane insertion and lateral mobility of synthetic amphiphilic signal peptides in lipid model membranes. *Biochim. Biophys. Acta*. 1071:123–148.

Tsuji, A., and S. Ohnishi. 1986. Restriction of the lateral motion of band 3 in the erythrocyte membrane by the cytoskeleton network: dependence on spectrin association state. *Biochemistry*. 25:6133–6139.

Tsuji, A., K. Kawasaki, S. Ohnishi, H. Merkle, and A. Kusumi. 1988. Regulation of band 3 mobilities in erythrocyte ghost membranes by protein association and cytoskeletal meshwork. *Biochemistry*. 27: 7447–7452.

Vaz, W. L. C., M. Criado, V. M. C. Madeira, G. Schoellmann, and T. M. Jovin. 1982a. Size dependence of the translational diffusion of large integral membrane proteins in liquid-crystalline phase lipid bilayers. A study using fluorescence recovery after photobleaching. *Biochemistry*. 21:5608–5612.

Vaz, W. L. C., Z. I. Derzko, and K. A. Jacobson. 1982b. Photobleaching measurements of the lateral diffusion of lipids and proteins in artificial phospholipid bilayer membranes. *Cell Surface Rev.* 8:83–135.

Vaz, W. L. C., and D. Hallmann. 1983. Experimental evidence against the applicability of the Saffman-Delbrück model to the translational diffusion of lipids in phosphatidylcholine bilayer membranes. *FEBS Lett.* 152:287–290.

Vaz, W. L. C., F. Goodsaid-Zalduondo, and K. Jacobson. 1984. Lateral diffusion of lipids and proteins in bilayer membranes. *FEBS Lett.* 174:199–207.

Vaz, W. L. C., and M. Criado. 1985. A comparison of the translational diffusion of a monomer and an oligomer of the acetylcholine receptor protein reconstituted into soybean lipid bilayers. *Biochim. Biophys. Acta*. 819:18–22.

Vaz, W. L. C., R. M. Clegg, and D. Hallmann. 1985a. Translational diffusion of lipids in liquid crystalline phase phosphatidylcholine multibilayers. A comparison of experiment with theory. *Biochemistry*. 24:781–786.

Vaz, W. L. C., D. Hallmann, R. M. Clegg, A. Gambacorta, and M. DeRosa. 1985b. A comparison of the translational diffusion of a normal and a membrane-spanning lipid in $L_\alpha$ phase 1-palmitoyl-2-oleoylphosphatidylcholine bilayers. *Eur. Biophys. J.* 12:19–24.

Xu, X., R. Bittman, G. Duportail, D. Heissler, C. Vilcheze, and E. London. 2001. Effect of the structure of natural sterols and sphingolipids on the formation of ordered sphingolipid/sterol domains (rafts). *J. Biol. Chem.* 276:33540–33546.

Yuan, C., J. Furlong, P. Burgos, and L. J. Johnston. 2002. The size of lipid rafts: an atomic force microscopy study of ganglioside GM1 domains in sphingomyelin/DOPC/cholesterol membranes. *Biophys. J.* 82: 2526–2535.

Zacharias, D. A., J. D. Violin, A. C. Newton, and R. Y. Tsien. 2002. Partition of lipid-modified monomeric GFPs into membrane microdomains of live cells. *Science*. 296:913–916.